

# Development of Silicon Strip Detectors for a Medium Energy Gamma-Ray Telescope

F. Schopper, R. Andritschke, G. Kanbach, J. Kemmer, M.-O. Lampert, P. Lechner, R. Richter, P. Rohr, V. Schönfelder, L. Strüder and A. Zoglauer<sup>1 2 3 4 5</sup>

## Abstract

The Medium Energy Gamma-ray Astronomy (MEGA) telescope is a new instrument under development by the gamma-astronomy group at MPE. In MEGA, the primary photon interaction is recorded in a stack of double-sided silicon strip detectors (the tracker). A small prototype of the tracker is currently being assembled at MPE with 11 detector layers each consisting of 3x3 silicon wafers connected to low noise VLSI amplifiers. We report on the design, status and results of these prototype detectors. For photons of 122 keV, energy resolution of 15 keV FWHM and trigger threshold of 30 keV has been achieved.

## I. INTRODUCTION

Several new gamma-ray telescopes plan to use large-area semiconductor detectors and are currently under development in various research laboratories. The Max-Planck Institut für extraterrestrische Physik plans the Medium Energy Gamma Astronomy telescope (MEGA). MEGA will be the first astronomical instrument able to form images from both Compton- and pair creation events. The goal of MEGA is to improve sensitivity in the 0.5-50 MeV energy range by an order of magnitude over that of COMPTEL.

MEGA, sketched in Figure 1, consists of a silicon tracker and a calorimeter. The calorimeter is made of pixelated CsI-crystals with photodiode readout [1]. In this paper we describe in detail the silicon strip detectors used in the tracker.

In a Compton interaction, the incident photon scatters off an electron of the tracker material to which part of its energy is transferred. The recoil electron is tracked on its way through several layers of the silicon stack. The track information is used to suppress background by restricting the measurement uncertainty of individual photon detections to the “reduced event circle” (see Figure 1) [2]. The scattered photon is then stopped in the calorimeter and the scatter angle  $\varphi$  can be

<sup>1</sup>This work was supported by DLR under reference numbers 50TT 97389 and 50 OO 0002

<sup>2</sup>Florian Schopper, Robert Andritschke, Gottfried Kanbach, Volker Schönfelder, Lothar Strüder and Andreas Zoglauer are with the Max-Planck-Institut für Extraterrestrische Physik, Giessenbachstraße, 85740 Garching, Germany e-mail: fls@mpe.mpg.de

<sup>3</sup>Josef Kemmer and Peter Lechner are with KETEK GmbH, Am Isarbach 30, 85764 Oberschleißheim, Germany peter.lechner@hll.mpg.de

<sup>4</sup>Rainer Richter is with the Max-Planck-Institut für Physik, Föhringer Ring, 80805 München, Germany email: rar@hll.mpg.de

<sup>5</sup>Marie-Odile Lampert and Pierre Rohr are with EURISYS MESURES, Parc des Tanneries 1, chemin de la Rosaie, LINGOLSHEIM BP 311, F-67834 TANNERIES Cedex, France <http://www.eurisysmesures.com>

determined from the energies of the recoil electron and the secondary photon. The angular resolution of the instrument depends among other parameters heavily on the measurement of the energy of the recoil electron [3].

In pair creation events the direction of the incident photon is determined directly from the track information of the secondary particles [4]. The energy measurement is used as a second order correction if the energies are not equally distributed between the electron and the positron.

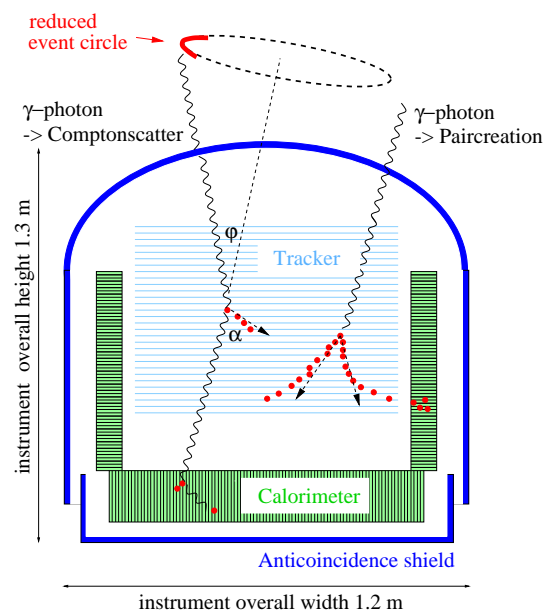


Figure 1: Overview of the MEGA instrument as planned to be mounted on a satellite. The tracker is a stack of 32 detector layers, each layer consisting of 4 smaller modules as described in this paper. The calorimeter surrounds the tracker to absorb the scattered photons or secondary particles. The anticoincidence shield made from plastic scintillator is used to veto against charged particles from the cosmic radiation.

## II. REQUIREMENTS FOR SILICON DETECTORS USED IN A COMPTON/PAIRCREATION TELESCOPE

For Compton- as well as pair creation telescopes, silicon strip detectors turned out to be the technology of choice, because they can cover large areas and volumes with a manageable number of readout channels. Compton telescopes pose several requirements for their detectors not commonly found in the requirements for silicon detectors used in HEP:

- Compared to the usual requirements for strip detectors, only moderate position resolution is necessary. The

angular resolution of low energy electron tracks is limited by small angle scattering within the first detector layer rather than by position resolution in the detectors. Therefore 0.5 mm position resolution with the possibility of improvement by centroiding for high energy tracks is sufficient.

- X and y position information must be available in each detector volume, so doublesided strip detectors are mandatory.
- Good energy resolution needs to be achieved as it translates directly into the angular resolution of the Compton telescope. A value of 15 keV FWHM energy resolution in the tracker introduces an angular error of  $1^\circ$  FWHM at an energy of the incident photon of 1 MeV. This is sufficient because the energy resolution of the calorimeter [1] is limited to  $\sim 30$  keV FWHM, which introduces a similar angular uncertainty. The energy measurement in each layer is also used to determine the direction of motion of the tracks [2]. Because the energy loss is subject to Landau fluctuations, an energy resolution of 15 keV is sufficient in this respect also.
- A trigger signal for each detected hit must be created which is used in time-coincidence with the calorimeter to form a first-level trigger. The trigger signals can also be used to form a second-level trigger which determines the track-length and thus rejects less significant events in the case of high event rates.
- The power consumption of the front end electronics has to be less than 10W/(kg Si). This makes it feasible to build an astronomical instrument with an effective area of about  $100 \text{ cm}^2$  @ 1MeV (corresponding to 5 kg Si).

### III. DETECTOR DEFINITION AND DESIGN

Following the requirements mentioned above, double sided silicon strip detectors were designed in the MPI Semiconductor Laboratory. The boundary conditions for the design were the following: An active area of  $60 \times 60 \text{ mm}^2$  with 128 orthogonal strips on each side with a strip-pitch of  $470 \mu\text{m}$ . The fabrication was to be done on 4" wafers of  $500 \mu\text{m}$  thick material. As will be explained later in more detail, the requirement for an energy resolution of 15 keV FWHM (resp.  $1763 \text{ e}^- \text{ ENC}$ ) restricts the acceptable leakage current to  $81 \text{ nA/channel}$  or  $3.4 \mu\text{A/wafer}$  if 3 wafers are concatenated.

#### A. Device Simulation

To evaluate the influence of the strip width on the strip capacitance and the depletion voltage, numerical simulations using the 2D device simulator TOSCA were performed. The simulation geometry used is shown in Figure 2. The n-strips are separated by a non-masked p-implantation ("p-spray"). The effective implanted dose can be varied locally by either keeping or removing a layer of silicon nitride on the wafer before implantation. The term "moderated p-spray" refers to a lower p-spray concentration along the border of the n-side

strips, thus reducing the strip capacitance and the electric field. The simulations showed that the capacitance is lowered by 10% if there is a  $10 \mu\text{m}$  gap between the n-strip and the full p-spray implant. The simulation results are summarized in

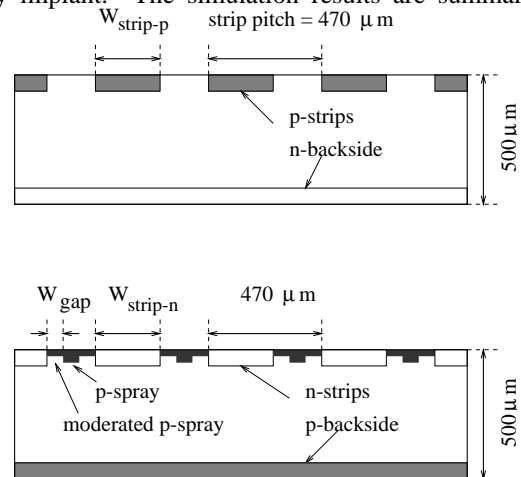


Figure 2: Cross section of the wafer geometry used in the simulation.

Table 1 for various strip widths on p- and n-side. The total strip capacitance  $C_{tot}$  can be separated into the capacitance to the neighbouring strips  $C_{neighbours}$ , of which 99% is related to the first neighbour, and the backplane capacitance.

Table 1

Results of detector simulations for p- and n-side strips. A strip pitch of  $470 \mu\text{m}$  and a wafer thickness of  $500 \mu\text{m}$  was used in the simulated

geometry			
p-side			
$W_{strip-p}$	$200 \mu\text{m}$	$300 \mu\text{m}$	$400 \mu\text{m}$
$C_{neighbours}$	11.5 pF	18.8 pF	23.0 pF
$C_{tot}$	16.6 pF	24.4 pF	28.8 pF
$V_{Dep}$	108 V	99 V	91 V
n-side			
$W_{strip-n}$	$200 \mu\text{m}$	$300 \mu\text{m}$	$400 \mu\text{m}$
$C_{neighbours}$	18.0 pF	21.5 pF	27.3 pF
$C_{tot}$	23.4 pF	27.2 pF	33.1 pF

#### B. Mask Layout

A width of  $300 \mu\text{m}$  for the p-side strips and  $200 \mu\text{m}$  for the n-side strips was chosen for production because it should result in similar electronic noise on both sides. The strips are AC-coupled by metal strips  $50 \mu\text{m}$  wide and 6-cm long, separated from the strip implant by insulating layers of silicon oxide ( $1500 \text{ \AA}$ ) and silicon nitride ( $900 \text{ \AA}$ ). For diagnostic reasons every 8th strip on each side has an additional ohmic contact.

Biasing of strips is achieved with the punch-through principle. The punch-through contacts are formed across a gap between the end of each strip and a common bias ring. The gap width is  $8 \mu\text{m}$  for the p-side respective  $12 \mu\text{m}$  for the n-side. The p-side bias ring is again surrounded by ten narrow guard rings designed to bring down the bias voltage applied to the innermost guard ring to zero at the crystal cut edge. Figure 3

shows the layout of the p-side with the bias ring and the guard ring structure.

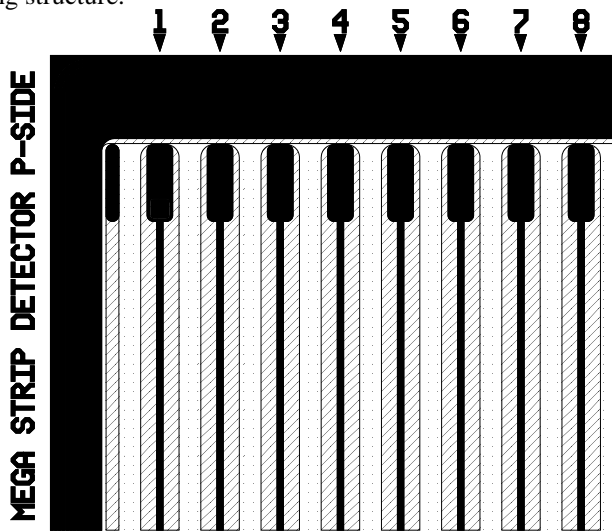


Figure 3: Plot of the layout of the p-side.

#### IV. PROPERTIES MEASURED ON WAFER LEVEL

These measurements were performed on a probe station before the wafers were diced.

##### A. Depletion Voltage

The voltage necessary to fully deplete the wafer was determined in two ways:

- The capacitance of reverse biased test diodes saturates as soon as the device is fully depleted.
- The current between one of the DC-coupled strips and the bias ring on the n-side is measured while applying a fixed voltage. This current is suppressed and finally switched off when the wafer is fully depleted from the p-side (Figure 4).

Both methods gave values between 40 and 60 V for all tested wafers. This corresponds to a very satisfying resistivity of the bulk material of 16 to 24 k $\Omega$ cm.

##### B. Punch-through Biasing

The characteristics of the punch-through biasing were measured by applying a voltage difference and measuring the current between one of the DC-coupled strips and the bias ring. The effective bias resistance depends on the leakage current flowing to that strip. It can be calculated from the slope of the I-V-curve shown in Figure 5 to be  $\sim 16$  M $\Omega$  on the p-side and  $\sim 40$  M $\Omega$  on the n-side at a leakage current of 1  $\mu$ A per wafer.

#### V. PRODUCTION AND YIELD

The production of the Wafers was done at EURISYS. A total of 171 Wafers were delivered to the MPI semiconductor laboratory for testing and qualification. Each strip was tested

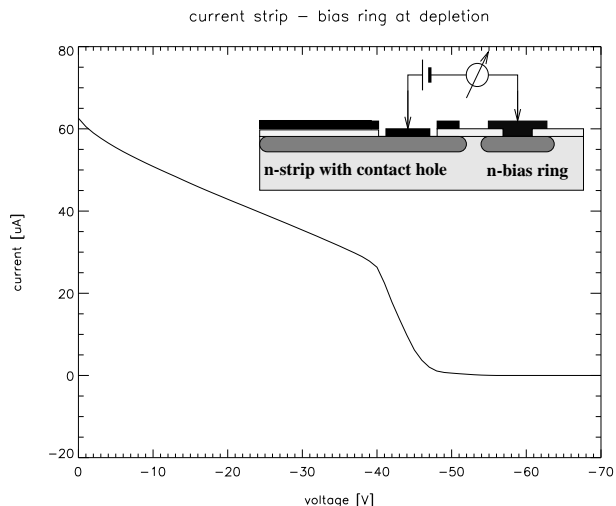


Figure 4: Suppression of the current between n-strip and n-side bias ring at full depletion.

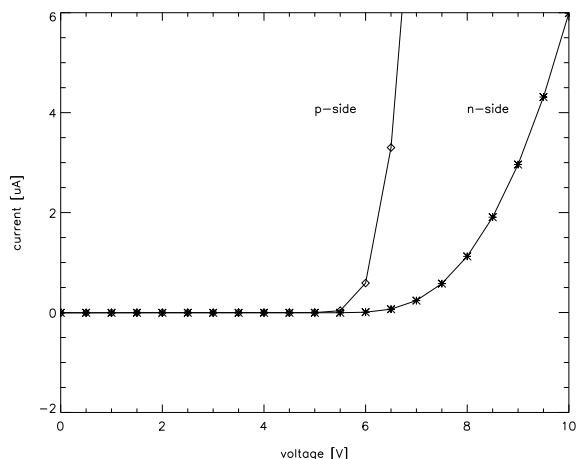


Figure 5: Punch through characteristics of the MEGA strip detector p- and n-side bias rings.

on a probe station to stand a voltage of 100 V across the coupling capacitors. 22% of the wafers had more than 2 shorted capacitors per wafer and were not used further. The leakage current of each wafer was measured by applying a voltage ramp from 0 to 100 V at  $\sim 25^\circ$  C ambient temperature. Figure 6 shows the distribution of the leakage currents at 60 V bias. 14% of all tested wafers showed leakage currents of more than 3.5  $\mu$ A and were not used either.

#### VI. READOUT ELECTRONICS

Each strip on the detector is connected via fan-in lines on a hybrid board to one channel of a frontend ASIC. This ASIC (TA1.1), which was developed by IDE<sup>6</sup>, is a 128 channel low noise/low power charge sensitive preamplifier-shaper circuit with simultaneous sample and hold, multiplexed analogue readout and calibration facilities. Each channel has in addition

<sup>6</sup>Integrated Detector & Electronics, Veritasveien 9, Box 315, N-1323 Høvik, Norway E-mail: ide@ideas.no

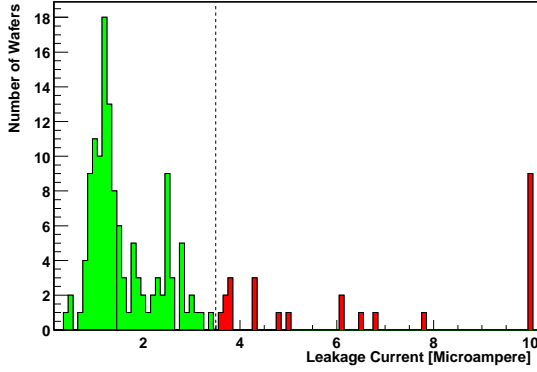


Figure 6: Leakage currents of all tested wafers at  $\approx 25^\circ\text{C}$  and 60 V bias. Only wafers with leakage currents below  $3.5 \mu\text{A}$  were mounted in the detectors.

its own level-sensitive discriminator following the shaper. It provides a trigger each time the signal in the given channel rises above the externally pre-settable threshold of the discriminator. The trigger outputs from all channels are OR'ed together on a common trigger output. Through a loadable bitmask it is possible to suppress the trigger of individual channels.

The TA1 shows a baseline noise of  $ENC_{Base} = 165 e^-$  and a noise slope of  $ENC_{slope} = 7 e^-/\text{pF}$  at a shaping time of  $2 \mu\text{s}$ . The power consumption has been measured to be only  $\sim 0.5 \text{ mW} / \text{channel}$ . The maximum linear range is 22 fC (500 keV in Si) if the full range is used for single polarity signals.

The ASICs on either side of the detectors refer to different ground potentials. Therefore the analog data and digital control signals are transmitted through optocouplers to the data acquisition system.

## VII. RESULTS

In the final configuration, each detector consists of a  $3 \times 3$  matrix of wafers with a border length of 18.6 cm. This arrangement requires the lowest possible number of readout channels for doublesided strip detectors. The wafers are glued with epoxy resin on a carrier structure made from PEEK which allows access to all bonding contacts on both sides. The two sides of the detectors are connected to identical hybrid boards of which one is mounted upside down as shown in Figure 7. The strips are concatenated by bond wires on the top and bottom sides to form a nearly continuous sensitive surface. Bias contacts are also concatenated.

### A. Readout Noise and Energy Resolution

One of the most important detector parameters for MEGA is the readout noise because it determines both the energy resolution and the angular resolution of the instrument. The noise is expected to be:

$$ENC^2 = (ENC_{Base} + ENC_{slope} * C_{tot})^2 + 2A \left( \frac{I_{leak}}{q} + \frac{kT}{qR} \right) \tau$$

with the filter coefficient  $A = 1.3$  for semigaussian shaping [5] and the filter time constant  $\tau = 2 \mu\text{s}$ . We find the average

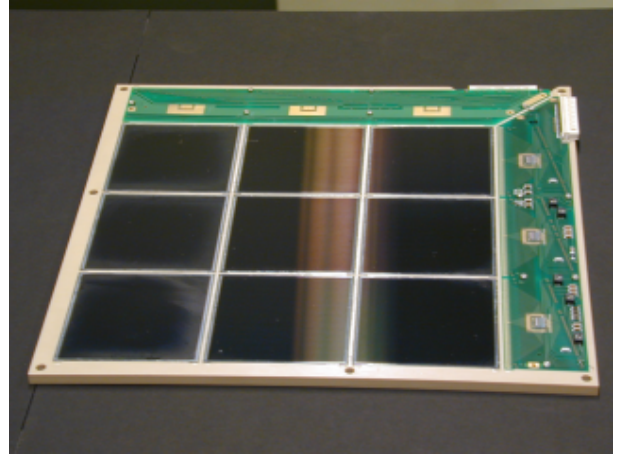


Figure 7: Photograph of one detector layer. P-side is on top with strips running from left to right which are connected to the hybrid on the right side. The second hybrid (top left) is flipped upside down and bonded to the strips on the bottom side.

leakage current of the first 4 layers to be  $30 \mu\text{A}$  per layer with all wafers mounted, glued and bonded. We make the assumption of a homogeneous distribution of currents over all strips and the assumption that  $1/3$  of the current is collected by the guard rings. This leads to  $52 \text{ nA}/\text{strip}$  if 3 wafers are concatenated and a contribution of  $1592 e^-$  ENC of this current to the overall noise. To evaluate the influence of strip length on noise, in one layer only one and two wafers were concatenated by bond wires on each side. Figure 8 shows the expected and measured ENC values for the three strip lengths. While the numbers fit reasonably well for the p-side, the increased noise on the n-side remains unexplained. While all data from both sides is used

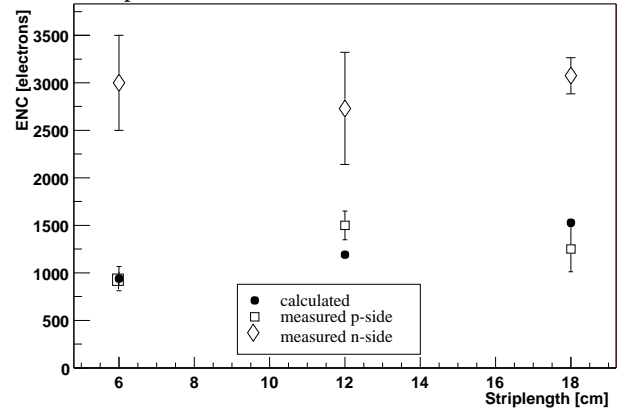


Figure 8: Equivalent noise charge for p- and n-side strips for a single wafer, two wafers concatenated and three wafers concatenated. The error bars indicate the standard deviation of the distribution over the strips.

to find matching energy deposits in the case of multiple hits, only the data from the p-side is used for energy measurements. Figure 9 shows a spectrum of a  $^{57}\text{Co}$  calibration source (122 and 136 keV). The common mode noise has been subtracted from the data before the noise was calculated. The average value of the common mode noise is only  $\sim 5 \text{ keV}$ . It is very important to keep the common mode noise low if self-triggered electronics

are used, because the common mode noise cannot be subtracted on the input of the trigger circuits.

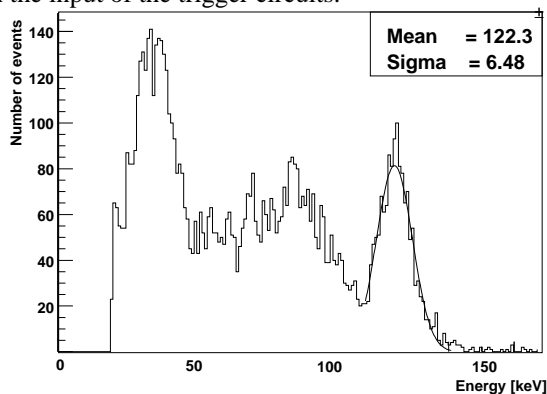


Figure 9: Spectrum of a  $^{57}\text{Co}$  calibration source (122 keV). X-ray fluorescence lines at  $\sim 35$  keV (from Cs and I) are detected also.

### B. Time Resolution

Time resolution is important for Compton telescopes because it determines the ratio of true coincident events to chance coincidences. In the TA chips (version 1.1) a simple level discriminator is used to derive the trigger from the shaped analogue signals. There is no compensation for pulseheight variations. Time resolution was measured relative to a plastic scintillator with constant fraction timing with a positron emitter ( $^{22}\text{Na}$ ) placed between the two detectors. Figure 10 shows the time distribution of trigger signals which is dominated by time-walk. The next version of the TA-chips will include a second shaper for each channel with a faster shaping time of  $\sim 100$  ns to reduce the timewalk variations.

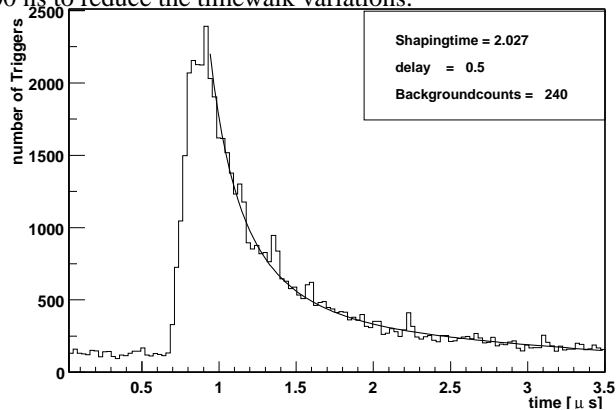


Figure 10: Time resolution for all strips of 4 layers. The thick line is a fit of the pulse height distribution (Compton distribution) transformed into the time domain by the output function of the CR-RC shaping.

### C. Position Resolution

The relatively large strip pitch of these detectors does not allow centroiding for most low energy events. If no interpolation is used, a picture such as in Figure 11 can be obtained with 122 keV photons. A small number of strips are insensitive due to higher noise level and their triggers have been blocked.

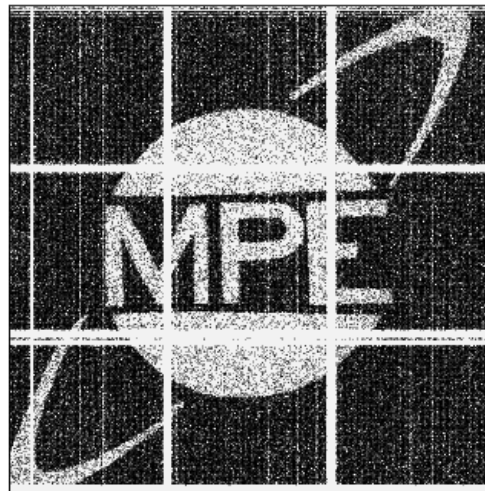


Figure 11: Projection of  $^{57}\text{Co}$  source (122 keV) through a lead mask. A window of 100-150 keV has been applied to the pulseheight signal. The trigger of some strips with increased noise levels have been switched off.

## VIII. CONCLUSIONS

Large area silicon strip detectors for space application have been designed, produced and tested. Equipped with self triggering readout electronics, X- and gamma-ray photons as well as charged particles can be detected. Calibration results of the MEGA instrument will be published in a separate paper.

The method of concatenating p- and n-side strips did not cause problems of any kind except for more difficult mounting and bonding.

## IX. REFERENCES

- [1] F. Schopper, R. Andritschke, H. Shaw, C. Nefzger, A. Zoglauer, V. Schönfelder, and G. Kanbach, "CsI calorimeter with 3-d position resolution," *Nuc. Inst. and Methods*, vol. 442, no. A, pp. 394–399, 2000.
- [2] T. Neill, F. Ait-Ouarmer, I. Schwarz, O. Turner, R. White, and A. Zych, "Compton recoil electron tracking with silicon strip detectors," *IEEE Trans. Nuc. Sci.*, vol. 39, 1992.
- [3] V. Schoenfelder et al, "Instrument Description and Performance of the Imaging Gamma-Ray Telescope COMPTEL aboard the Compton Gamma-Ray Observatory," *Astroph. J. Suppl. Series*, vol. 86, pp. 657–692, 1993.
- [4] G. Kanbach et al, "The project EGRET on NASA's Gamma-Ray Observatory GRO," *Space Science Reviews*, vol. 49, pp. 69–84, 1988.
- [5] E. Gatti P. Manfredi, *Processing the Signals from Solid-State Detectors in Elementary Particle Physics*, vol. 9, La Rivista del nuovo Cimento, 1986.